Observation of Anomalously Large Spectral Bandwidth in a High-Gain Self-Amplified Spontaneous Emission Free-Electron Laser

G. Andonian,[1] A. Murokh,[1] J. B. Rosenzweig,[1] R. Agustsson,[1] M. Babzien,[2] I. Ben-Zvi,[2] P. Frigola,[1] J. Y. Huang,[2] L. Palumbo,[3] C. Pellegrini,[1] S. Reiche,[1] G. Travish,[1] C. Vicario,[3] and V. Yakimenko[2]

[1]*Department of Physics and Astronomy, University of California Los Angeles, Los Angeles, California 90095, USA*
[2]*Accelerator Test Facility, Brookhaven National Laboratory, Upton, New York 11973, USA*
[3]*Universita degli Studi di Roma "La Sapienza", Via Antonia Scarpa 14, Rome, 00161, Italy*

(Received 14 March 2005; published 25 July 2005)

Observation of ultrawide bandwidth, up to 15% full-width, high-gain operation of a self-amplified spontaneous emission free-election laser (SASE FEL) is reported. This type of lasing is obtained with a strongly chirped beam ($\delta E/E \sim 1.7\%$) emitted from the accelerator. Because of nonlinear pulse compression during transport, a short, high current bunch with strong mismatch errors is injected into the undulator, giving high FEL gain. Start-to-end simulations reproduce key features of the measurements and provide insight into mechanisms, such as angular spread in emitted photon and electron trajectory distributions, which yield novel features in the radiation spectrum.

DOI: 10.1103/PhysRevLett.95.054801 PACS numbers: 41.60.Cr, 41.75.−i, 41.85.Ew, 42.60.Jf

High-brightness, ultrashort duration x-ray radiation from the self-amplified spontaneous emission free-election laser (SASE FEL) promises to be an invaluable tool for broad sections of the scientific community. Coherent light sources which extend into the x-ray regime will allow investigations at the time and length scales of atomic processes. For example, such a source will enable biological sampling (single molecule diffraction) [1] and atomic structural dynamics studies. Current proposals [2,3] to construct single-pass high-gain x-ray SASE FELs will generate Ångstrom wavelength radiation, providing the spatial resolution desired for scientific applications. However, these sources are designed to operate at hundred femtosecond pulse lengths [4], with a clear demand to push to shorter time scales, down to the few fs regime.

A scenario to obtain such ultrashort pulses by creating and manipulating frequency-chirped FEL output has been proposed [5]. In the scheme's first stage, an energy-chirped electron beam injected into the undulator produces a frequency-chirped output. This radiation is passed through a monochromator and a narrow bandwidth is transmitted to the second stage. The narrow band pulse then acts as a seed for gain over a short longitudinal region of the beam with energy corresponding to injected frequency. In order to test aspects of this scheme, the VISA II experiment has been designed to operate with the highest chirp allowable at the Brookhaven National Laboratory Accelerator Test Facility (BNL ATF). In this experiment, the aim is to produce and measure strongly chirped SASE FEL radiation based on electron beam chirping.

To understand the present measurements, we first review some results of the VISA (Visible to Infrared SASE Amplification) FEL experiment. In 2001, VISA successfully demonstrated a high-gain SASE FEL and saturation within the 4 m undulator at 840 nm [6]. An atypical electron bunch compression mechanism was responsible for creating beam conditions which produced high-gain lasing. The large second-order longitudinal time dispersion, T_{566} [7], in combination with off-energy operation, yielded pulse compression, increasing the peak current from 55 to 240 A. The self-consistent evolution of the electron beam was studied using a start-to-end simulation code suite that models the beam and its interactions from inception at a photocathode to the FEL exit. The electron beam dynamics in the injector sections are modeled with PARMELA [8], the electron beam transport is analyzed with ELEGANT [9], and the evolution of the beam and FEL radiation in the undulator is computed with GENESIS 1.3 [10]. The reproduction of important aspects of the radiation, as well as the identification of the bunch compression mechanism, were significant achievements of the simulations. The benchmarking of the simulations against the experimental knowledge of the beam production and transport in VISA allows reliance on the same modeling tools to analyze microscopic aspects of the present measurements.

Although the original bunch compression mechanism facilitated high-gain lasing, it restricted the management of the electron beam properties prior to injection into the undulator. The VISA II experiment seeks to preserve the electron beam chirp linearization of the longitudinal compression process, through the use of sextupole magnets at high horizontal dispersion points in the dogleg transport to the undulator. This method has been shown to mitigate second-order effects in longitudinal transport, particularly by reducing T_{566} to a negligible value [11,12]. The initial, nearly linear, electron beam chirp applied at the linac, can then be preserved and even modestly enhanced (to increase the peak current) before injection into the undulator.

As a prelude to the implementation of transport linearization, a set of experiments performed without sextupoles have been made on the existing VISA facilities at the ATF. These measurements employ a highly chirped, post-

linac pulse, which, through nonlinear longitudinal compression, achieves conditions that generate robust FEL amplification.

This transitional experiment indeed demonstrates unanticipated and previously unobserved phenomena. In particular, an extremely large relative bandwidth of the FEL radiation, up to 15% full-width (FW, width above noise floor), at high gain is observed, as illustrated by Fig. 1. The large spectral width is accompanied by an anomalously wide far-field angular radiation pattern, similar to that observed in Ref. [6], but even more pronounced in angle. In this Letter, we present these results, as well as simulations that reproduce the most striking aspects of the radiation measurements.

Relevant aspects of the VISA experimental setup utilized in the present measurements are discussed in detail in Refs. [6,13]. The 70 MeV photoinjector electron source is followed by a 20° dogleg transport line that delivers beam to the undulator. The dogleg contains an adjustable collimator, termed the high energy slits (HES), at a high energy dispersion point. Measurements of electron beam size and transmitted fraction at the HES are used to determine the transmitted beam's mean energy and energy spread. Because of the time-energy chirp imparted by the linac, the 500 pC electron beam possesses a 2.8% energy spread, as observed impinging on the HES. Of this initial charge, approximately 330 pC (1.7% energy spread) propagates through the HES to the undulator.

As in Ref. [6], the compression process in the dogleg is monitored by measuring the coherent transition radiation (CTR) [14] emitted from an insertable foil. The CTR energy is peaked when the beam's energy-time chirp is chosen to optimize the bunch compression. Measurements from the CTR monitor, along with energy and energy spread observed at the HES, allow the benchmarking of the simulation model to the experiment.

The modeling of the beam transport indicates that the peak current in the electron pulse after nonlinear compression reaches up to 300 A. GENESIS simulations show that the lasing peak contains 25–30 pC of charge and is short in duration compared to the electron bunch length. Unlike the original VISA conditions, the compression is insensitive to injection phase fluctuations arising from either rf or photocathode laser timing jitter. This is due to the large energy spread in the initially chirped beam [Fig. 2(a)], which guarantees that a component of the beam is compressed, as the injection errors are much smaller than the initial bunch length of 10 ps. The electron beam at undulator injection displays a highly nonlinear longitudinal phase space as a result of the second-order effects in the transport line [Fig. 2(b)].

The observed FEL radiation at high gain displays an extraordinary wavelength distribution. The spectrum is notable for its double peak structure, having a mean value of the relative full-width (FW) bandwidth of 12%. The average measured SASE radiated energy is approximately 2 μJ, which is less than an order of magnitude of the saturation energy of the initial VISA experiment. The dual-spike spectral structure indicates the presence of two distinct lasing modes. The FEL output is much more stable than in earlier VISA runs, due to the enhanced reproducibility of the electron beam pulse compression process.

The anomalous width of the wavelength spectrum is observed whenever high-gain conditions are present. In Fig. 3 the distribution of the spectral rms width is shown for the radiation shots yielding the top 10% of SASE energy. This distribution's peak is at 21 nm rms width, corresponding to 12% FW (2.3% rms). Shots up to 33 nm rms width (15% FW, 3.6% rms) are observed. For comparison, the relative width observed previously at VISA was 2.4% FW (0.5% rms).

The simulations with GENESIS provide insight into the underpinnings of the unusual FEL amplification. First and foremost, the FEL reaches the onset of saturation, consistent with the experimental comparison to previous VISA data. This lasing condition shows that the high current obtained through compression ensures high-gain SASE

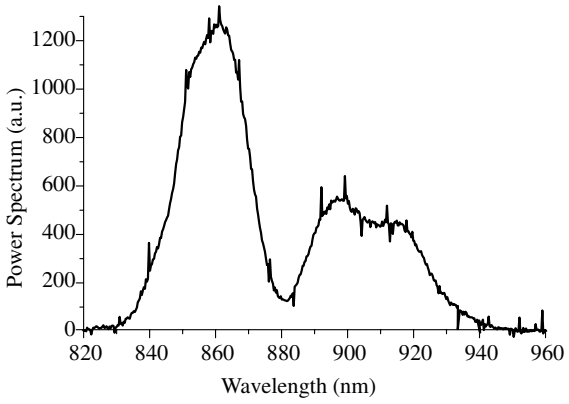

FIG. 1. Sample shot of observed SASE FEL spectrum, showing anomalously wide bandwidth.

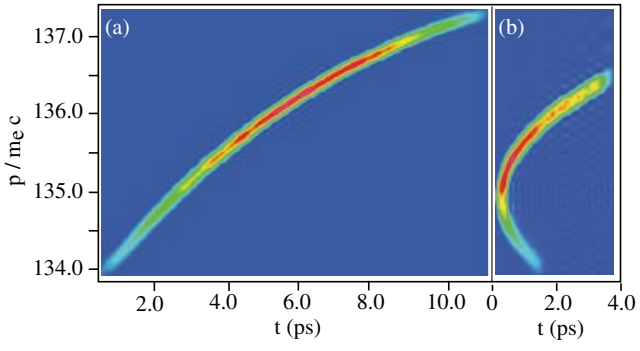

FIG. 2 (color online). Simulated electron beam longitudinal phase space at (a) linac exit (PARMELA output, ELEGANT input) and (b) at undulator injection (ELEGANT output). Pulse compression, from 10 to 4 ps, and clipping at the slits is evident.

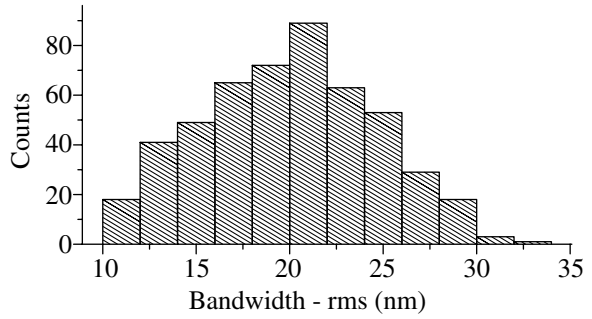

FIG. 3. Distribution of measured rms spectral bandwidth (501 highest collected energy shots).

FEL operation and outweighs any possible degradation of the slice emittance due to the large energy spread and residual dispersion.

The simulations also reproduce key facets of the observed wavelength spectrum, namely, the large bandwidth and double spiked structure (Fig. 4). The GENESIS results show that the secondary spike observed in the spectra is due to the amplification of an off-axis, large angular-spread mode. They further indicate that this mode is excited by the nonideal beam centroid and envelope motion as the electrons perform betatron oscillations in the undulator's quadrupole focusing lattice.

While the electron beam as a whole is aligned to the undulator axis, the lasing core's centroid is misaligned, undergoing $\sim$300 μm oscillations. Further, the rms envelope of the lasing core is strongly mismatched to the focusing lattice, resulting in variations between 30 and 90 μm in x and 40 and 70 μm in y. As seen in Fig. 5, there is a notable correlation between the oscillations in beam radius and the periodic growth in the spectral bandwidth.

To aid in understanding the effects that produce the observed spectra, we refer to the FEL resonance relation,

$$\lambda_r = \frac{\lambda_u}{2\gamma^2}\left[1 + \frac{K^2 + K_q^2}{2} + (\gamma\theta)^2\right]. \quad (1)$$

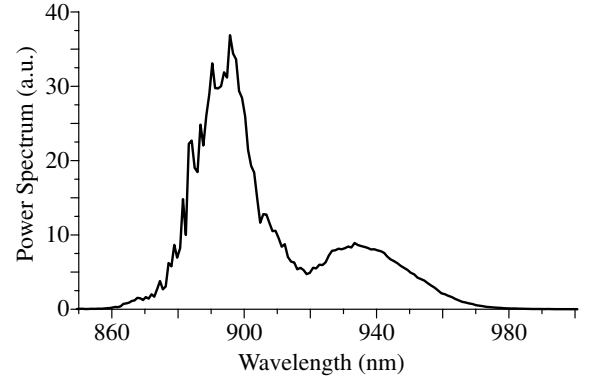

FIG. 4. Sample SASE wavelength spectrum given by GENESIS simulations for the modeled experimental conditions.

Here λ_r is the radiation wavelength, λ_u is the undulator period, $\gamma = E/m_e c^2$ is the normalized energy of the electron beam, K is the normalized undulator field parameter, K_q accounts for effects on the resonance due to quadrupole focusing, and θ is the observation angle of the radiation with respect to the electron beam trajectory. Energy spread has a negligible impact on the simulated spectral bandwidth. Even when GENESIS is run with all particles set to near equal energy, there is no notable change in the simulated FEL spectrum.

The redshifting of the radiation arises mainly from the last two terms in Eq. (1). The first of these terms indicates the degradation of the longitudinal velocity due to transverse motion, which has two sources in this experiment. The first component of this term is quantified by the undulator parameter; $K = 2\pi e B_u/m_e \lambda_u c = 1.26$, as the peak magnetic field $B_u = 0.72$ T for the VISA undulator. Because of the large excursions in the undulator focusing lattice, additional transverse motion causes a redshift in the radiated wavelength. The bend in the electron trajectory due to the quadrupole fields, which have a square-wave form, yields an effective undulator parameter of $K_q \simeq eB'\Delta x L_q/\sqrt{2}\pi m_e c$, where B' is the quadrupole gradient, Δx is the amplitude of oscillation, and L_q is the focusing period. For VISA parameters, $K_q \simeq 0.16$, corresponding to a maximum trajectory angle of 1.2 mrad. The maximum predicted fractional redshifting of the resonant wavelength due to this effect is 1.5%, corresponding to an rms spectral spread of 0.38%, when averaged over a betatron period. We note that such broadening effects, due to changes in the electron longitudinal velocity, have been studied [15,16] recently in a similar context, that of Thomson-scattering sources.

Large amplitude betatron motion and its associated horizontal angles contribute not only this direct source of radiation redshift, but also allow greater coupling to off-axis (higher spatial-order) emission modes. In turn, this off-axis emission provides the dominant source of radiation redshifting (greater than the effect due to angles in the electron trajectory). As in previous VISA results [6], the far-field angular spectrum is typically hollow, but has maximum intensity at much larger θ, in excess of

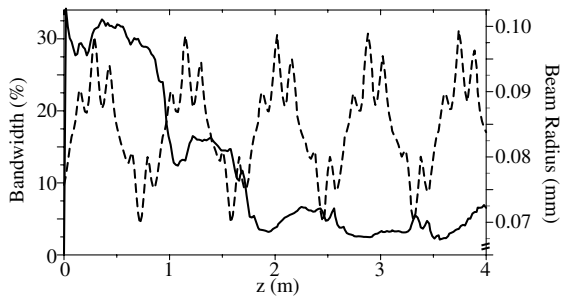

FIG. 5. rms radiation bandwidth (solid line) and electron beam lasing core radius (dashed line) along the undulator.

2 mrad. The redshifting associated with θ is $\sim$4.2%, corresponding to the relative shift of the long wavelength peak compared to the short wavelength (on-axis) peak (Fig. 1). The relative shift in λ at an off-axis observation angle deduced from Eq. (1) is $\Delta\lambda/\lambda_r \simeq (\gamma^2\theta^2)/(1 + \frac{K^2}{2})$. In the simulations, $(\theta^2)_{\mathrm{rms}} = 1.8 \times 10^{-6}$ mrad^2, corresponding to an rms wavelength spread of 2.0%. Accounting for all sources of spectral broadening discussed above, the total rms wavelength spread expected under our experimental conditions is 2.2%, in good agreement with observations.

The production of the measured bandwidth's anomalous aspects through off-axis emission is correlated to oscillations in rms beam size. A bi-Gaussian transverse distribution of radiators with rms widths $\sigma_{x,c}$ and $\sigma_{y,c}$ may emit coherently into angles as large as $\theta_c = (\lambda_r/4\pi) \times \sqrt{\sigma_{x,c}^{-2} + \sigma_{y,c}^{-2}}$. For the beam sizes indicated in Fig. 5, this prediction yields θ_c in the range of 1.7–2.5 mrad, consistent with the observed emission angles. On the other hand, Fig. 5 shows that when the transverse beam size is smallest (the maximum coherent angle is largest) the bandwidth rapidly decreases. This behavior is accompanied in simulations by a notable increase in the gain. The connection between the gain and bandwidth variations is that the on-axis, short wavelength mode gain is enhanced by the increase in beam density when the transverse beam size is small, resulting in ''gain guiding'' [17]. However, the redshifted mode gain is not as strongly enhanced, due to its wider angular emission, and the radiation bandwidth diminishes. As the FEL begins to saturate, gain guiding is no longer effective, and the ratio of on-axis radiation to that of higher order modes is reduced. The FEL enters a final, pronounced period of bandwidth growth, yielding the observed state of large spectral spread.

Further work is ongoing to obtain a more complete understanding of the physics of large-angle coherent emission in an FEL. Initial follow-on experiments have yielded even richer off-axis mode structures, including not only hollow ring mode profiles, but spiral shapes as well. In order to explore the angular emission effects in a high-gain FEL, a radiation diagnostic is being developed to image the far-field intensity along a slit. The wavelength spectrum is dispersed in the direction normal to the slit by gratings to produce a double-differential energy spectrum, $d^2I/d\omega d\theta$; this allows direct comparison to the form of common approaches to analysis of radiative processes [18]. Initial data show the existence of several modes and verify the overall parabolic shape of the radiation intensity in (θ, ω) space.

The results presented here have general implications for the possible observable emission spectra in FELs. Indeed, ultrahigh bandwidth emission, while not desirable from the viewpoint of absolute brightness (or for VISA II), may be beneficial for selected applications. For example, in material absorption studies, this operating regime mitigates the sensitivity of a narrow absorption-line experiment to fluctuations of the FEL central frequency; one may scan a range of absorption wavelengths with a single pulse. The high bandwidth also allows for more flexibility in use of the radiation pulse, as it may be manipulated (by, e.g., monochromators) without changing the running parameters of the linac. This option would be attractive for a multiple-user facility.

Generation of an anomalously wide angular distribution may also be desirable in an x-ray FEL [2,3], where the natural divergence of the on-axis FEL radiation is so small and the intensities are so large, that the generated pulse requires a very long drift [2] before it can be manipulated with x-ray optics. Coupling of FEL emission into off-axis modes, through mechanisms uncovered in the present work, may be a useful maneuver for reducing the length and complexity of an x-ray transport line.

This work was performed with support from U.S. Department of Energy Contract No. DE-FG-98ER45693 and Office of Naval Research Contract No. N000140210911.

[1] R. Neutze *et al.*, Nature (London) **406**, 752 (2000).
[2] M. Cornacchia *et al.*, Linac Coherent Light Source Design Study Report No. SLAC-R-521, 1998 (unpublished).
[3] TESLA-FEL, Deutsches Elektronen Synchrotron 2001–05, Technical Report No. DESY-01-011, 2001 (unpublished).
[4] C. Pellegrini and J. Stohr, Nucl. Instrum. Methods Phys. Res., Sect. A **500**, 33 (2003).
[5] C. Schroeder *et al.*, J. Opt. Soc. Am. B **19**, 1782 (2002).
[6] A. Murokh *et al.*, Phys. Rev. E **67**, 066501 (2003).
[7] K. Brown, Stanford Linear Accelerator Center Technical Report No. SLAC-R-075, 1982 (unpublished).
[8] L. M. Young and J. H. Billen, Los Alamos National Laboratory Report No. LA-UR-96-1835, 2000 (unpublished).
[9] M. Borland, Advanced Photon Source Report No. LS-287, 2000 (unpublished).
[10] S. Reiche, Nucl. Instrum. Methods Phys. Res., Sect. A **429**, 243 (1999).
[11] J. England *et al.*, Phys. Rev. ST Accel. Beams **8**, 012801 (2005).
[12] P. Piot *et al.*, Phys. Rev. ST Accel. Beams **6**, 030702 (2003).
[13] A. Tremaine *et al.*, Phys. Rev. Lett. **88**, 204801 (2002).
[14] A. Murokh *et al.*, Nucl. Instrum. Methods Phys. Res., Sect. A **507**, 417 (2003).
[15] G. A. Krafft, Phys. Rev. Lett. **92**, 204802 (2004).
[16] J. Gao, Phys. Rev. Lett. **93**, 243001 (2004).
[17] S. Krinsky and L. H. Yu, Phys. Rev. A **35**, 3406 (1987).
[18] J. D. Jackson, in *Classical Electrodynamics* (Wiley, New York, 1999), 3rd ed..